Research Article

Journal of Environmental Nanotechnology

Rice Husk Ash–derived Silica Nanoparticles as Eco-friendly Sensitizers for Enhanced Solar Photovoltaic Performance

Chamundeeswari Munusamy[1*], Mohanapriya Purushothaman[1], Chitrakala Subramanian[1], Mary Nancy Flora Rayappan[2]and Ramya Ravi[3]

[1]Department of Biotechnology, St. Joseph's College of Engineering, OMR, Chennai, TN, India
[2]Department of Chemical Engineering, Vel Tech High Tech Dr. Rangarajan Dr. Sakunthala Engineering College, Avadi, Chennai, TN, India
[3]Department of Petrochemical Engineering, JCT College of Engineering and Technology, Coimbatore, TN, India
Received: 23.02.2026 Accepted: 04.03.2026 Published: 30.03.2026
*chamundeeswari@gmail.com

ABSTRACT

Nanostructured silica has attracted considerable attention due to its high surface area, tunable physicochemical properties, and wide applicability in electronic, catalytic, and biomedical systems. In this study, high-purity silica nanoparticles were synthesized from rice husk ash through a thermo-chemical route, providing a value-added strategy for agricultural waste utilization. The novelty of this work lies in the development of rice husk-derived silica nanoparticles as sensitizing materials for photovoltaic applications. Structural and morphological properties of the synthesized material were characterized using X-ray diffraction (XRD), Fourier transform infrared spectroscopy (FT-IR), scanning electron microscopy coupled with energy-dispersive X-ray spectroscopic, transmission electron microscopy (TEM), Brunauer–Emmett–Teller analysis and X-ray fluorescence (XRF) spectroscopy. FT-IR spectra showed characteristic peak at 779 and 1112 cm^{-1}, confirming the formation of an amorphous silica network, while XRD exhibited a broad diffraction peak at $2\theta = 21.57°$, indicating the amorphous nature of the material. The XRF analysis confirmed ~100% silica purity, and TEM images revealed uniform particles with sizes below 10 nm and mesoporous morphology. Photovoltaic performance evaluation demonstrated enhanced voltage generation under sunlight irradiation compared with green-synthesized carbon nanoparticles and the conventional dye Coomassie Brilliant Blue. These findings suggest that rice husk-derived silica nanoparticles can serve as promising eco-friendly sensitizing materials for sustainable photovoltaic applications.

Keywords: Rice husk; Silica nanoparticles; Muffle furnace; Xerogels; Siloxane.

1. INTRODUCTION

Nanotechnology is a rapidly advancing interdisciplinary field encompassing research, development, and industrial applications. It involves the design and fabrication of materials and devices through precise control of matter at the nanometer scale (1–100 nm), where unique physical, chemical, mechanical, and electronic properties emerge (Aitken, 2004). At this scale, materials exhibit characteristics that differ significantly from their bulk counterparts due to high surface-to-volume ratios, quantum confinement and energy level quantization (Roduner, 2006). These properties enable the development of advanced functional materials for applications in electronics, optics, catalysis, environmental remediation, and renewable energy technologies.

Among various nanomaterials, silicon-based materials and silica nanoparticles (SiNPs) have attracted considerable attention because of their stability, large surface area, tunable morphology, and favorable optical and electronic properties. These characteristics make silica nanomaterials particularly promising for photovoltaic and photoelectrochemical applications, including dye-sensitized solar cells. In such systems, nanostructured silica can enhance light absorption, facilitate dye adsorption, and improve charge separation efficiency during solar-to-electrical energy conversion (Karuppuchamy *et al.*2006). Ultrafine silica particles often exhibit improved photocatalytic activity compared to bulk materials due to their increased surface area and size-dependent physicochemical properties (Ohno *et al.*2009). The thermal and mechanical properties of silicon materials were tabulated in Table 1.

Silicon is the second most abundant element in the Earth's crust; however, it rarely occurs in its elemental form and is typically found as silica and silicate minerals. Crystalline silicon was first synthesized by Deville in 1854, although its unique electronic properties became widely understood only after the development of quantum mechanics in the early twentieth century (Bullis, 1998). Silicon belongs to

Group 14 of the periodic table and crystallizes in a cubic lattice structure in which each atom is covalently bonded to four neighboring atoms. Crystalline silicon exhibits an indirect bandgap structure in which the maximum of the valence band (E_v) and the minimum of the condition band (E_C) occur at different momentum states. Consequently, photogenerated charge carriers must travel longer diffusion distances to reach the p–n junction in photovoltaic devices, which imposes strict requirements on material purity and crystal perfection for efficient solar energy conversion (Goetzberger *et al.* 2003). The electronic configuration of silicon exhibits $1s^2\ 2s^2\ 2p^6\ 3s^2\ 3p^2$ orbitals. Under atmospheric pressure, silicon crystallizes as cubic lattice structure, where silicon atoms are covalently bonded to four nearest neighbouring atoms, as illustrated in Fig. 1.

Table 1. Thermal and mechanical properties of silicon

Property	Value
Atomic weight (g/mol)	28.085
Atomic density (atoms/cm^3)	5.22×10^{22}
Melting point (°C)	1410
Boiling point (°C)	2355
Density (g/cm^3)	2.329
Heat of fusion (KJ/g)	1.8
Heat of vaporization at melting point (KJ/g)	16
Percent contraction at melting (%)	9.5

Silica nanoparticles are generally water-dispersible, chemically inert, non-toxic, and relatively easy to synthesize using cost-effective methods (Metin *et al.*2012). They typically exhibit low bulk density (0.04–0.1 g cm^{-3}) and high specific surface areas ranging from 200–300 m^2 g^{-1} (Napierska *et al.*2010). The physicochemical properties of these nanomaterials strongly depend on particle size and surface structure. As particle size decreases, the proportion of surface atoms increases significantly, leading to changes in interatomic spacing, lattice strain, and surface energy (Christian *et al.*2008; Brydson and Hammond, 2005). These nanoscale characteristics play a critical role in determining the optical, catalytic, and electronic behavior of silica-based materials.

In recent years, increasing attention has been directed toward the sustainable synthesis of silica nanoparticles from agricultural waste materials. Several agro-industrial residues contain significant quantities of silica and can serve as low-cost precursors for nanomaterial production. For example, cordierite powders have been synthesized using rice husk ash as a silica source via sol–gel techniques (Naskar and Chatterjee, 2004). Similarly, sugar beet bagasse has been utilized for silica nanoparticle synthesis through laser ablation methods, producing particles with sizes ranging from 38 to 190 nm, significantly smaller than those obtained by conventional alkali extraction processes (San*et al.*2014). Silica xerogel has also been prepared from corn cob ash through alkali extraction followed by acid neutralization, producing amorphous silica containing siloxane and silanol functional groups.

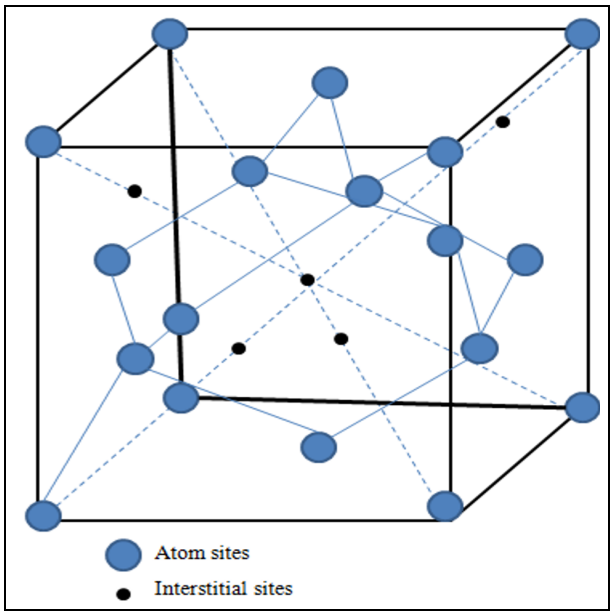


Fig. 1: Crystalline structure of silicon

Among these resources, rice husk is one of the most abundant agricultural byproducts, accounting for approximately 20–25% of the total dry weight of paddy rice (Chang *et al.*2002). Rice husk primarily consists of lignocellulosic components and contains approximately 15–28 wt% silica (Chen *et al.*2013). Despite its high silica content, rice husk is often disposed of through open-field burning, which results in environmental pollution and greenhouse gas emissions (Lim *et al.*2012). The utilization of rice husk as a raw material for silica nanoparticle synthesis therefore represents a sustainable approach that simultaneously addresses waste management and value-added material production.

However, despite the increasing interest in silica nanomaterials, the development of environmentally sustainable and economically viable methods for producing silica nanoparticles from agricultural waste remains limited, particularly for applications in photovoltaic and energy-conversion systems. Therefore, the present study focuses on the synthesis of silica nanoparticles from rice husk and the evaluation of their structural and functional properties for potential solar energy applications.

2. EXPERIMENTAL METHODS

2.1 Chemicals

Silica nanoparticles were synthesized from a natural precursor, rice husk, which was collected from local farmers in Villupuram District after the harvest season. The chemicals required for the synthesis of mesoporous SiNPs, including sodium hydroxide and cetyltrimethylammonium bromide (CTAB), were procured from Spectrum Fine Chemicals, India. Hydrochloric acid, sulfuric acid, and butanol were purchased from Merck, India. All chemicals were of analytical grade and were used as received without further purification.

2.2 Sample Collection and Treatment

Rice husk, an agricultural by-product rich in silica, was selected as the precursor material based on its availability, low cost, and high silicon content. The collected rice husk was thoroughly washed with deionized water to remove adhering dust and impurities and then air-dried at room temperature. To eliminate organic components and residual contaminants, the dried material was subjected to thermal treatment in a muffle furnace. Initially, the sample was pre-heated at 300 °C for 1 hour to remove moisture and volatile organic compounds. Subsequently, the temperature was increased to 800 °C at a heating rate of 10 °C min^{-1} and maintained for 2 hours to obtain rice husk ash (RHA), following previously reported procedures (Srivastava*et al.*2013; Chamundeeshwari *et al.*2013). The calcination process resulted in the formation of silica-rich ash through oxidation reactions within the furnace environment.

$$SiC + 2O_2 \rightarrow SiO_2 + CO_{2(g)} \quad \ldots (1)$$

2.3 Preparation of Sodium Silicate Solution

Silica was extracted from the obtained rice husk ash using a modified alkali extraction method (Samsudin*et al.*2009). Briefly, 20 g of RHA was mixed with 250 mL of 1 M NaOH solution and heated to boiling under continuous stirring for 1 hour to produce sodium silicate solution according to the following reaction:

$$nSiO_2 + 2NaOH \rightarrow Na_2O.nSiO_2 + H_2O \quad \ldots (2)$$

After completion of the reaction, the solution was cooled to room temperature and filtered through Whatman No. 41 filter paper (particle retention 20–25 µm) to remove insoluble residues and carbonaceous impurities.

2.4 Siloxane Formation

The purified sodium silicate solution was gradually titrated with 1 N HCl until the pH reached neutral conditions. During this process, silicic acid species were generated, initiating hydrolysis and condensation reactions that led to the formation of siloxane (Si–O–Si) linkages.

$$H_2SiO_4^{2-} \xrightarrow{H^+} H_3SiO_4^- \xrightarrow{H^+} H_4SiO_4 \xrightarrow{H^+} H_5SiO_4^+ \quad \ldots (3)$$

At higher pH levels, the dominant species are $H_2SiO_4^{2-}$ and $H_3SiO_4^-$, whereas at near-neutral conditions, $H_3SiO_4^-$ and H_4SiO_4 become predominant and initiate polymerization. The condensation of silanol groups produces siloxane bridges and releases hydroxyl ions, resulting in a gradual increase in pH during the reaction (Iler, 1979).

$$H_3SiO_4^- + H_4SiO_4 \rightarrow (OH)_3Si - O - Si(OH)_3 + OH^- \quad \ldots (4)$$

The resulting gel was allowed to age for 12–24 hours to strengthen the three-dimensional siloxane network. After aging, the gel was washed several times with deionized water, mechanically dispersed into slurry form, and centrifuged at 10,000 rpm for 10 min to separate the solid phase.

2.5 Preparation of Silica Xerogels

A 2 wt% CTAB solution was prepared using a water–butanol mixture (1:1 v/v) as solvent. The sodium silicate extract obtained from the centrifuged pellet was added to the CTAB solution and stirred continuously. The mixture was heated at 60 °Cfor 8 hours under constant stirring, following the procedure described by Le *et al.* (2013), leading to the formation of silica gel. The gel was then dried to obtain silica xerogels.

$$Si(C_4H_{10}O)_4 + H_2O \rightarrow Si(OH)(C_4H_{10}O)_3 + C_4H_9OH \quad \ldots (5)$$

$$Si(OH)(C_4H_{10}O)_3 + Si(OH)(C_4H_{10}O)_3 \rightarrow (C_4H_{10}O)_3(Si - O - Si)(C_4H_{10}O)_3 + H_2O \quad \ldots (6)$$

2.6 Synthesis of SiNPs

The silica xerogels were washed repeatedly with a butanol–water mixture (1:1 v/v) to remove residual impurities. Subsequently, 0.5 mol L^{-1} sulfuric acid was added to initiate hydrolysis to condensation reactions at pH 4, leading to the formation of nano silica gel. The semi-liquid gel was separated by centrifugation and collected as pellets.

$$NaOH + SiO_2 \rightarrow Na_2SiO_3 + H_2O \quad \ldots (7)$$

$$Na_2SiO_3 + H_2SO_4 \rightarrow SiO_2 + Na_2SO_4 + H_2O \quad \ldots (8)$$

The obtained pellets were then calcined at 550 °C for 4 hours to remove the surfactant template completely and obtain purified SiNPs. The overall yield of silica nanoparticles from rice husk ash was approximately 78 ± 3% (w/w).

$$Si(OC_4H_{10})_4 \rightarrow SiO_2 + 2(C_4H_{10})_2O \quad \ldots (9)$$

2.7 Characterization of Synthesised SiNPs

The structural and physicochemical properties of the synthesized silica nanoparticles were analyzed using multiple characterization techniques. Fourier transform infrared (FT-IR) spectroscopy was used to identify functional groups and confirm silica formation. X-ray powder diffraction (XRD) was employed to determine the crystallographic structure and degree of crystallinity. X-ray fluorescence (XRF) analysis was used to determine elemental composition and purity.

The morphology and elemental distribution of the nanoparticles were examined using scanning electron microscopy coupled with energy-dispersive X-ray spectroscopy (SEM–EDS). Particle size and morphology were further analyzed using transmission electron microscopy (TEM). For TEM analysis, samples were dispersed in ethanol using ultrasonic treatment and drop-cast onto a carbon-coated copper grid. Particle size distribution was determined by measuring at least 100 individual nanoparticles using ImageJ software, and the average particle size was calculated.

2.8 Enhanced Solar Panel Radiation Sensitizer by Green Synthesised SiNPs

To investigate the photovoltaic sensitization potential of the synthesized silica nanoparticles, electrical conductivity measurements were performed under controlled laboratory conditions. Carbon nanoparticles (CNPs) were prepared from cotton wick soot generated by burning cotton wicks soaked in 40 mL of gingelly (*Sesamum indicum*) oil in an earthenware vessel. The soot deposited on the inner surface of the vessel was carefully collected and stored in sterile containers to avoid contamination.

The collected carbon nanoparticles were mixed with silica nanoparticle xerogels in a 1:1 weight ratio and stirred for 30 min to obtain a homogeneous composite suspension. Electrical measurements were performed for three different samples such as SiNPs, SiNPs mixed with Coomassie Brilliant Blue (CBB) dye and SiNPs doped with CNPs.

Electrical potential measurements were carried out using a digital multimeter (SEW DT860D) with a two-probe electrode configuration. The probes were positioned at a fixed distance of 1 cm on the sample-coated glass substrate. The electrical response was measured under presence and absence of sunlight irradiation. All measurements were performed in triplicate (n = 3), and the results were expressed as mean ± standard deviation to ensure reproducibility and minimize experimental error.

3. RESULTS AND DISCUSSION

Silica nanoparticles were successfully synthesized from rice husk using a sol–gel approach, demonstrating an effective waste-to-value strategy for producing functional nanomaterials from agricultural residues. The synthesized SiNPs were subjected to comprehensive physicochemical characterization to determine their structural, morphological, and electrical properties.

3.1 FT-IR Analysis

The Fourier Transform Infrared (FT-IR) spectrum of the synthesized SiNPs is shown in Fig. 2, which confirms the formation of silica through characteristic vibrational peaks. Broad absorption peaks observed at 779 cm^{-1} and 1112 cm^{-1} correspond to the symmetric and asymmetric stretching vibrations of Si–O–Si bonds, respectively, indicating the presence of a siloxane network typical of amorphous silica structures. Similar peak assignments have been reported for biosynthesized silica nanoparticles in previous studies (Nayak and Bera, 2010; Javed *et al.*2011).

The absorption peak located at 1640 $cm^{-1}$is attributed to the bending vibration of surface hydroxyl groups (Si–OH) associated with adsorbed water molecules on the silica surface. These silanol groups are commonly observed in mesoporous silica materials and play an important role in surface reactivity and functionalization (Javed *et al.*2011).

In addition, the peak detected at 2860 $cm^{-1}$is associated with siloxane-related vibrations, further confirming the formation of a silica framework. The observed FT-IR spectral features are consistent with an earlier report for rice husk-derived amorphous silica nanoparticles (Le *et al.* 2013).

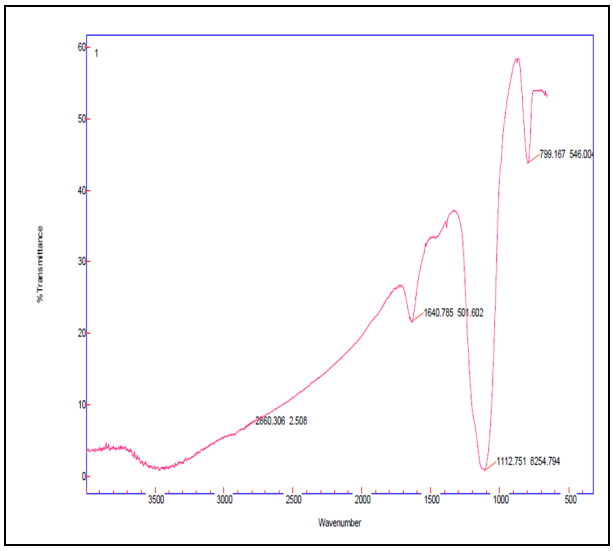


Fig. 2: FT-IR analysis of synthesized SiNPs

3.2 X-Ray Diffraction (XRD) Analysis

The crystalline characteristics of the synthesized SiNPs were analyzed using X-ray diffraction and the corresponding diffraction pattern is presented in Fig. 3. The diffractogram exhibits a broad peak centered at $2\theta \approx 21.57°$, which is a characteristic feature of amorphous silica. Such broad diffraction patterns arise from the absence of long-range atomic order in amorphous materials (Kamath and Proctor, 1998).

The presence of this diffuse peak confirms that the silica produced from rice husk ash predominantly exists in amorphous form, which is desirable for several applications including catalysis, adsorption, and photovoltaic materials due to its higher surface reactivity compared with crystalline silica. The estimated crystallite size calculated using the Scherrer equation ranged from 0.24 to 3.02 nm, indicating the formation of nanostructured silica domains within the amorphous matrix.

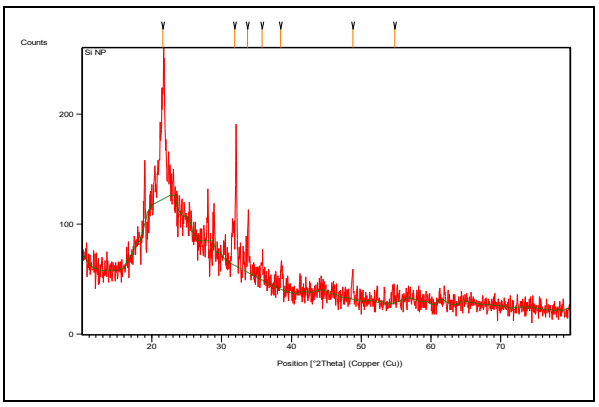


Fig. 3: X-Ray diffractogram of synthesized SiNPs

3.3 X-Ray Fluorescence Analysis

The elemental composition of the rice husk ash and the synthesized silica nanoparticles was analyzed using X-ray fluorescence spectroscopy, as shown in Fig. 4. The results indicate that rice husk ash initially contained approximately 91.80% SiO_2, whereas the purified product obtained after the modified extraction process exhibited an increased silica content of 93.52% SiO_2.

This improvement in silica purity confirms the effectiveness of the modified Affandi extraction method in removing metallic and non-metallic impurities present in the raw ash. The obtained purity level is consistent with previously reported values for silica derived from agricultural waste sources (Umamaheswaran and Batra, 2008).

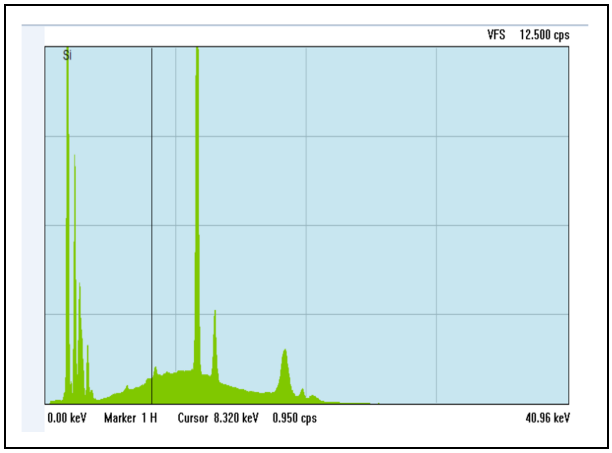


Fig. 4: XRF spectrum of synthesized SiNPs

3.4 Morphological Analysis using SEM–EDX

The surface morphology of the synthesized SiNPs was examined using scanning electron microscopy. The micrographs presented in Fig. 5 reveal heterogeneous particle structures with varied geometries, including spherical, prismatic, and fibrous morphologies. The presence of such mesoporous and irregular surface structures suggests a high surface area, which is advantageous for applications requiring enhanced surface interactions. Elemental analysis performed using energy-dispersive X-ray spectroscopy confirmed that silicon and oxygen were the dominant elements, verifying the successful synthesis of silica nanoparticles (Fig. 6). Minor signals corresponding to carbon and oxygen are likely associated with adsorbed atmospheric species and the sample preparation procedure used during SEM analysis. If correlated with surface area analysis, the observed porous morphology is expected to contribute to a high BET surface area, which is a typical feature of silica nanoparticles synthesized *via* sol–gel process.

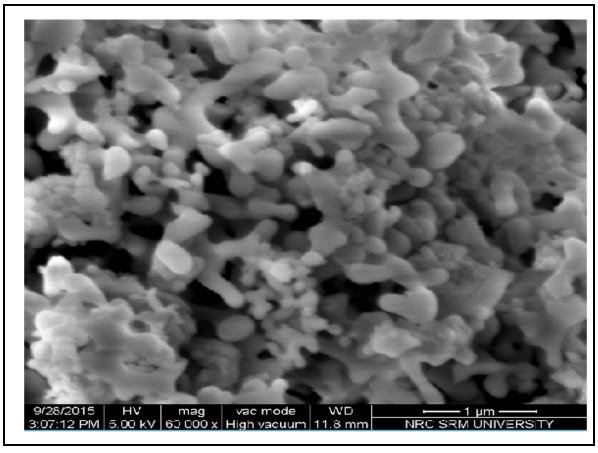


Fig. 5: SEM image of synthesized SiNPs

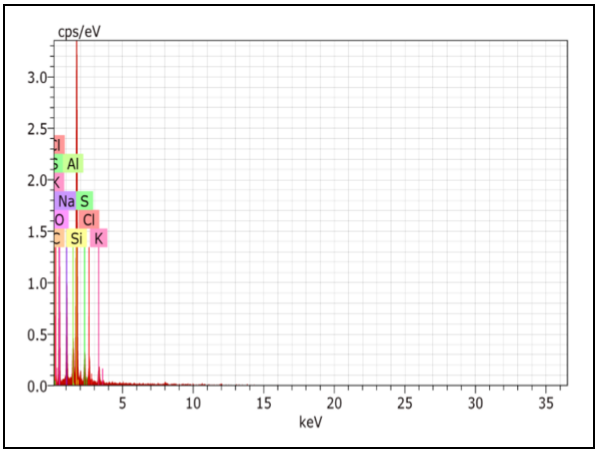


Fig. 6: EDX-micrograph of synthesized SiNPs

3.5 Transmission Electron Microscopy

The detailed particle morphology and size distribution of the synthesized silica nanoparticles were analyzed using transmission electron microscopy (Fig. 7). The TEM images reveal that the nanoparticles are predominantly spherical and well-dispersed, with an average particle size ranging between 2–5 nm.

Such nanoscale dimensions significantly increase the surface-to-volume ratio, which is beneficial for applications involving surface interactions, including catalysis, sensing, and light-responsive materials.

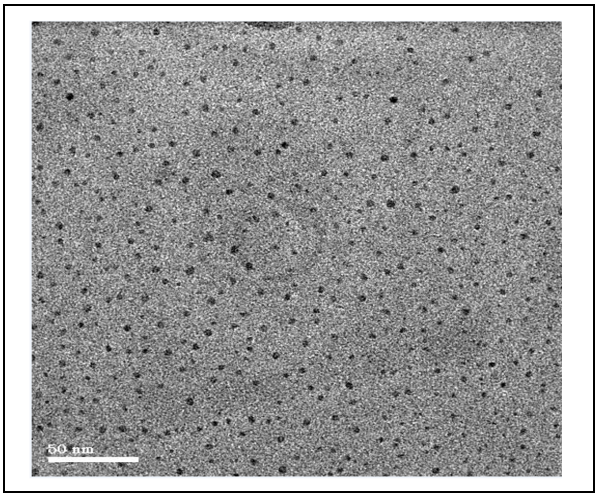


Fig. 7: TEM analysis of synthesized SiNPs

3.6 Electrical Response under Sunlight Irradiation

To explore the potential photovoltaic relevance of the synthesized SiNPs, electrical potential measurements were performed using three different formulations: pure SiNPs, SiNPs combined with CBB dye and SiNPs doped with carbon nanoparticles. The measurements were conducted under both dark conditions and sunlight exposure. It was noticed that the voltage values measured in digital multimeter represent electrical potential differences rather than direct electrical conductivity measurements. Nevertheless, these measurements provide an indication of the photo-responsive electrical behaviour of the prepared materials when exposed to solar radiation.

The results summarized in Table 2 show that pristine SiNPs exhibited a potential of 176 mV under dark conditions, which increased to 185 mV after 1 hour of sunlight exposure, corresponding to approximately 5% enhancement in electrical response. The digital multimeter shows a voltage value of approximately 176 mV, indicating that silica nanoparticles exhibit a measurable photo-induced electrical response when exposed to sunlight. When the silica nanoparticles are combined with the dye CBB, the voltage recorded is around 157 mV. The dye acts as a light-absorbing sensitizer, capturing photons and contributing to electron excitation. The composite system containing silica nanoparticles doped with carbon nanoparticles generates a voltage of approximately 173 mV, suggesting improved charge transport due to the conductive nature of carbon nanoparticles (Fig. 8 a-c). After exposure to sunlight, the voltage increases to about 185 mV, indicating enhanced electrical potential due to photoactivation of the silica nanoparticle system. The SiNP–CBB mixture records approximately 174 mV, demonstrating an increase in voltage compared with the initial measurement, likely due to improved photon absorption and charge separation. The SiNP–CNP composite exhibits a voltage value of approximately 178 mV, confirming that the addition of conductive carbon nanoparticles contributes to enhanced electron transport and electrical response (Figu.8 d-f).

These results suggest that the presence of light-absorbing components, such as dye molecules or conductive CNPs may enhance the photo-induced charge generation and transfer within the silica-based system.

Table 2. Conductivity measurement of SiNPs and SiNPs with dyes before and after exposure to sunlight

Environmental Conditions	Pure Silica (mV)	Silica + CBB (mV)	Silica + CNPs (mV)
Normal Room Temperature (Absence of Sunlight)	176	157	173
Presence of Sunlight	185	174	178

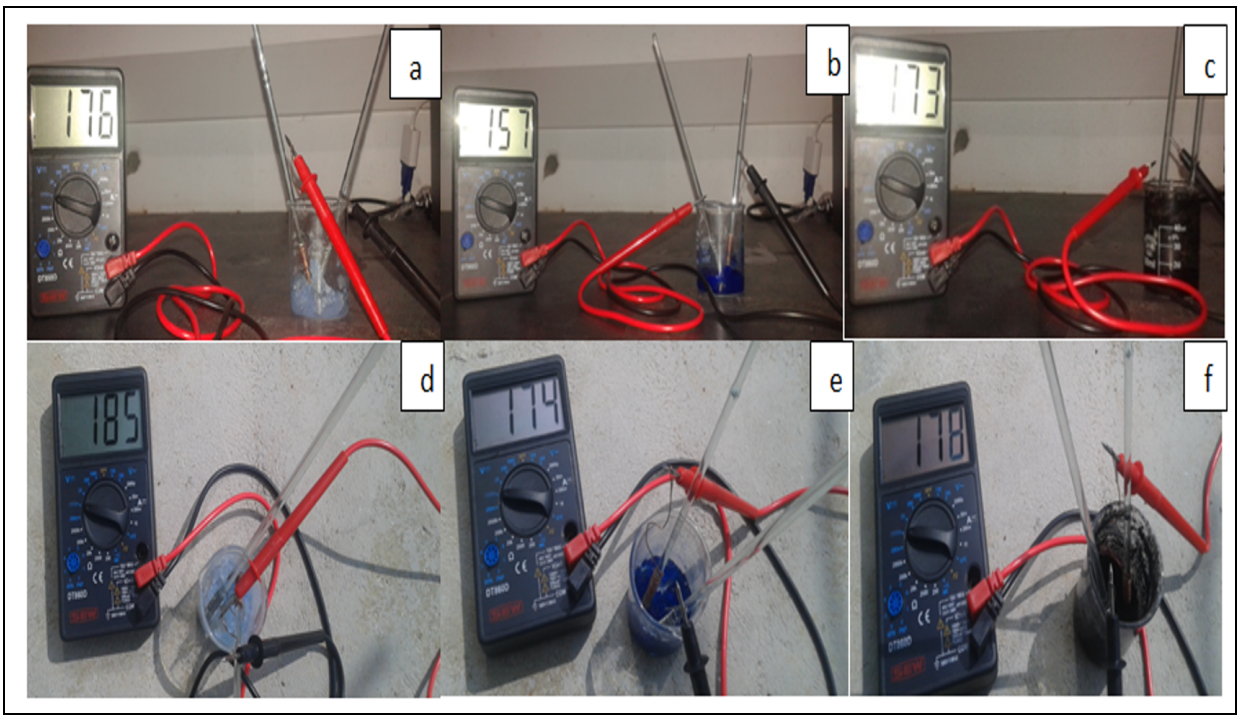


Fig. 8: Measurement of conductance for SiNPs using multimeter (a, d) (SiNPs alone), (b, e) (SiNPs + CBB), (c, f) (SiNPs + CNPs) in the presence (a–c) and absence (d–f) of sunlight

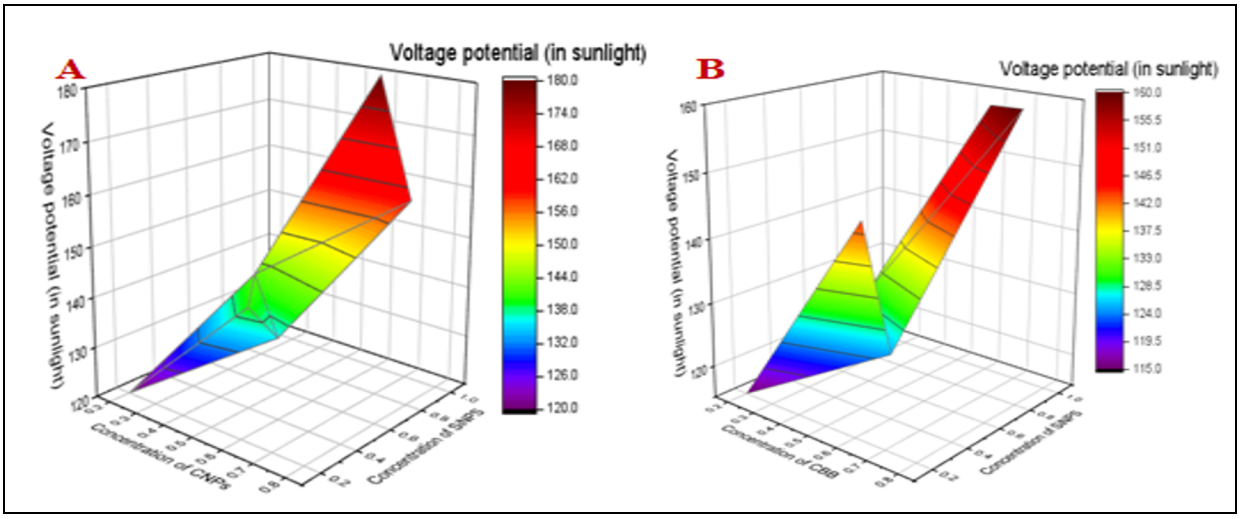


Fig. 9: Surface response plot of voltage potential under sunlight with concentration of (A) synthesized SiNPS and CNPs and (B)synthesized SiNPS and CBB

3.7 Photovoltaic Conductance Property

The three-dimensional surface plots represent the relationship between nanoparticle concentration and the resulting electrical potential. In Fig. 9A, the incorporation of CNPs with silica nanoparticles results in a progressive increase in voltage potential as the concentration of the composite increases. This improvement can be attributed to the enhanced charge transport properties of carbon nanoparticles, which facilitate electron mobility and improve photo-induced electrical response under sunlight. In Fig. 9B, silica nanoparticles combined with the dye CBB also exhibit an increase in voltage potential with increasing concentration. The dye molecules act as light-absorbing sensitizers, improving photon capture and contributing to enhanced photo-generated charge separation. Comparative analysis of the two systems indicates that both CNP and dye sensitization improve the photo-responsive electrical behavior of silica nanoparticles. However, the SiNP–CNP composite demonstrates slightly better electrical response due to the conductive nature of carbon nanoparticles, which facilitates efficient electron transport. These observations suggest that rice

husk-derived silica nanoparticles can function as supporting matrices for light-harvesting components, offering potential applications in low-cost photovoltaic and photoelectrochemical energy systems

4. CONCLUSION

The present study demonstrates a waste-to-wealth strategy by synthesizing silica nanoparticles from rice husk ash through a sol–gel process for potential solar energy applications. Characterization results confirmed the successful formation of nano silica. FT-IR analysis revealed characteristic Si–O–Si stretching vibrations at 779 and 1112 cm^{-1}, confirming the formation of a silica network. XRD analysis showed a broad diffraction peak at $2\theta \approx 21.57°$, indicating the predominantly amorphous nature of the synthesized silica. XRF results demonstrated a high silica purity exceeding 93% SiO_2, while SEM analysis revealed heterogeneous surface morphology. TEM imaging confirmed predominantly spherical nanoparticles with particle sizes in the range of approximately 2–5 nm. Electrical measurements indicated that the synthesized SiNPs generated a voltage potential of 176 mV under dark conditions, increasing to 185 mV after sunlight exposure, while SiNPs composites with carbon nanoparticles produced up to 178 mV, demonstrating enhanced photo responsive electrical behaviour. The improved electrical response can be attributed to the light-scattering ability of mesoporous SiNPs and the enhanced charge transport provided by conductive carbon nanoparticles, which together facilitate more efficient photon capture and electron mobility under solar irradiation. Future research should focus on integrating these SiNP-based materials into dye-sensitized solar cells, conducting long-term photovoltaic stability and efficiency testing, and optimizing nanoparticle doping ratios to further enhance charge transport and solar energy conversion performance.

DATA AVAILABILITY

The data used in this research are available from the corresponding author upon request.

AUTHOR CONTRIBUTION

Chamundeeswari Munusamy: conceptualization, writing, review and editing, funding acquisition, supervision; Mohanapriya: Manuscript draft preparation and background work; Chitrakala: experimental analysis and investigation, writing and original draft preparation; Mary Nancy Flora-Manuscript writing, review and editing; Ramya – writing, review, editing and background work.

FUNDING

This research received no specific grant from any funding agency in the public, commercial, or not-for-profit sectors.

CONFLICTS OF INTEREST

The authors declare that there is no conflict of interest.

COPYRIGHT

This article is an open-access article distributed under the terms and conditions of the Creative Commons Attribution (CC BY) license (http://creativecommons.org/licenses/by/4.0/).

REFERENCES

Aitken, R. J., Creely, K. S. and Tran, C. L., Nanoparticles: An Occupational Hygiene Review, *HSE Books,*274(2004).

Brydson, R. M. and Hammond, C., Generic methodologies for nanotechnology: Classification and fabrication, *Nanoscale Sci. Technol.*, 48–55(2005).

Bullis, M. W., Handbook of Semiconductor Silicon Technology*, S.R.L. Publications*, Italy (1998).

Chamundeeshwari, M., Sastry, T. P., Lakshmi, B. S., Senthil, V. and Agostinelli, E., Iron nanoparticles from animal blood for cellular imaging and targeted delivery, *Biochimica et Biophysica Acta*, 1830(4), 3005–3010(2013). https://doi.org/10.1016/j.bbagen.2012.12.031

Chang, F. W., Tsay, M. T. and Kuo, M. S., Effect of thermal treatments on catalyst reducibility in nickel supported on RHA-Al_2O_3 systems, *Thermo chimica Acta*, 386(2), 161–172(2002). https://doi.org/10.1016/S0040-6031(01)00771-7

Chen, H. R., Wang, W. X., Martin, J. C., Oliphant, A. J., Doerr, P. A., Xu, J. F., DeBorn, K. M., Chen, C. X. and Sun, L. Y., Extraction of lignocellulose and synthesis of porous silica nanoparticles from rice husks, *ACS Sustain. Chem. Eng.*, 1(2), 254–259(2013). https://doi.org/10.1021/sc300115r

Christian, P., Von der Kammer, F., Baalousha, M. and Hofmann, T., Nanoparticles: Structure, properties, preparation and behaviour in environmental media, *Ecotoxicol.*, 17(5), 326–343(2008). https://doi.org/10.1007/s10646-008-0213-1

Goetzberger, A., Hebling, C. and Schock, H., Photovoltaic materials: History, status and outlook, *Mater. Sci. Eng. R: Rep.*, 40(1), 1–46(2003). https://doi.org/10.1016/S0927-796X(02)00092-2

Iler, R. K., *The Chemistry of Silica*. Wiley-Interscience, *New York* (1979).

Javed, S. H., Shah, F. H. and Manasha, M., Extraction of amorphous silica from wheat husk using $KMnO_4$, *J. Facul. Eng. Technol.*, 18, 39–46(2011).

Kamath, S. R. and Proctor, A., Silica gel from rice hull ash: Preparation and characterization, *Cereal Chem.*, 75, 484–487(1998). https://doi.org/10.1094/CCHEM.1998.75.4.484

Karuppuchamy, S., Jeong, J., Amalnerkar, D. P. and Minoura, H., Photoinduced hydrophilicity of titanium dioxide thin films prepared by cathodic electrodeposition, *Vacuum*, 80(5), 494–498(2006). https://doi.org/10.1016/j.vacuum.2005.06.005

Le, V. H., Thuc, C. N. H. and Thuc, H.H., Synthesis of silica nanoparticles from Vietnamese rice husk by sol–gel method, *Nanoscale Res. Lett.*, 8, 58(2013). https://doi.org/10.1186/1556-276X-8-58

Lim, J. S., Manan, Z. A., Alwi, S. R. W. and Hashim, H., A review on utilisation of biomass from rice industry as a renewable energy source, *Renewable Sustain. Energy Rev.*, 16(5), 3084–3094(2012). https://doi.org/10.1016/j.rser.2012.02.051

Metin, C., Bonnecaze, R. and Nguyen, Q., The viscosity of silica nanoparticle dispersions in permeable media, *Appl. Rheology*, 21, 53–63(2012).

Napierska, D., Thomassen, L.C., Lison, D., Martens, J.A. and Hoet, P.H., The nanosilica hazard: Another variable entity, *Particle Fib. Toxicol.*, 7, 39(2010). https://doi.org/10.1186/1743-8977-7-39

Naskar, M.K. and Chatterjee, M., A novel process for the synthesis of cordierite ($Mg_2Al_4Si_5O_{18}$) powders from rice husk ash and other silica sources, *J. European Ceramic Soc.*, 24(13), 3499–3508(2004). https://doi.org/10.1016/j.jeurceramsoc.2003.11.029

Nayak, J. P. and Bera, J., Preparation of silica aerogel by ambient pressure drying using rice husk ash, *Trans. Ind. Ceram. Soc.*, 68, 1–4(2010).

Ohno, T., Itoh, H., Hisao, S., Takeshi, M. and Tagawa, S., Size effect of TiO_2–SiO_2 nanohybrid particles, *Mater. Chem. Phy.*, 113, 119–123(2009). https://doi.org/10.1016/j.matchemphys.2008.07.034

Roduner, E., Size matters: Why nanomaterials are different, *Chem. Soc. Rev.*, 35(7), 589–592(2006). https://doi.org/10.1039/B502142C

Samsudin, A., Setyawan, H., Winardi, S., Purwanto, A. and Balgis, R., Production of high purity silica xerogels from bagasse ash, *Adv. Powder Technol.*, 20(5), 468–472(2009). https://doi.org/10.1016/j.apt.2009.03.008

San, N.O., Kurşungöz, C., Tümtaş, Y., Yaşa, O., Ortaç, B. and Tekinay, T., Novel One-step synthesis of silica nanoparticles from sugar beet bagasse by laser ablation and their effects on growth of freshwater algae, *Particuology*, 17, 29–35(2014). https://doi.org/10.1016/j.partic.2013.11.003

Srivastava, K., Shringi, N., Devra, V. and Rani, A., Pure silica extraction from perlite: Characterization and affecting factors, *Int. J. Innov. Res. Sci. Eng. Technol.*, 2(7), 2936–2942(2013).

Umamaheswaran, K. and Batra, V.S., Physico-chemical characterization of Indian biomass ashes, *Fuel*, 87(6), 628–638(2008). https://doi.org/10.1016/j.fuel.2007.05.045